


## Dynamo Effect and Turbulence in Hydrodynamic Weyl Metals

Victor Galitski,<sup>1</sup> Mehdi Kargarian,<sup>2</sup> and Sergey Syzranov<sup>1,3</sup>

<sup>1</sup>*Joint Quantum Institute, Department of Physics, University of Maryland, College Park, Maryland 20742-4111, USA*

<sup>2</sup>*Department of Physics, Sharif University of Technology, Tehran 14588-89694, Iran*

<sup>3</sup>*Physics Department, University of California, Santa Cruz, California 95064, USA*

 (Received 7 June 2018; published 25 October 2018)

The dynamo effect is a class of macroscopic phenomena responsible for generating and maintaining magnetic fields in astrophysical bodies. It hinges on the hydrodynamic three-dimensional motion of conducting gases and plasmas that achieve high hydrodynamic and/or magnetic Reynolds numbers due to the large length scales involved. The existing laboratory experiments modeling dynamos are challenging and involve large apparatuses containing conducting fluids subject to fast helical flows. Here we propose that electronic solid-state materials—in particular, hydrodynamic metals—may serve as an alternative platform to observe some aspects of the dynamo effect. Motivated by recent experimental developments, this Letter focuses on hydrodynamic Weyl semimetals, where the dominant scattering mechanism is due to interactions. We derive Navier-Stokes equations along with equations of magnetohydrodynamics that describe the transport of a Weyl electron-hole plasma appropriate in this regime. We estimate the hydrodynamic and magnetic Reynolds numbers for this system. The latter is a key figure of merit of the dynamo mechanism. We show that it can be relatively large to enable observation of the dynamo-induced magnetic field bootstrap in an experiment. Finally, we generalize the simplest dynamo instability model—the Ponomarenko dynamo—to the case of a hydrodynamic Weyl semimetal and show that the chiral anomaly term reduces the threshold magnetic Reynolds number for the dynamo instability.

DOI: [10.1103/PhysRevLett.121.176603](https://doi.org/10.1103/PhysRevLett.121.176603)

The dynamo effect is a beautiful astrophysical phenomenon, first proposed by Larmor in 1919 [1], that is believed to be responsible for generating and sustaining magnetic fields in galaxies, stars, and planets, including the Sun and Earth [2]. There exist a large variety of different dynamo mechanisms [2–4] that all share the same key ingredient—hydrodynamic motion of an electrically conducting gas, fluid, or plasma. The dynamo theory deals with the hydrodynamic motion of a conductive medium focusing on the possibility of self-generating and self-sustaining magnetic fields, whose presence has been observed in astrophysical bodies.

As detailed below, the underlying equations of the theory are the Navier-Stokes equations, describing the hydrodynamic motion of the medium, coupled to the Maxwell equations of electromagnetism. In the nonrelativistic limit, they give rise to equations of magnetohydrodynamics (MHD). These are complicated nonlinear equations, and their exact solutions represent a great challenge. However, both the solutions of simplified MHD models [e.g., kinematic dynamos, with predetermined velocity fields  $\mathbf{u}(\mathbf{r}, t)$ ] and qualitative arguments [2] suggest that the dynamo action is possible when the terms enhancing the magnetic field [e.g., the induction term  $\nabla \times (\mathbf{u} \times \mathbf{B})$ ] overwhelm the magnetic diffusion term  $\eta_m \Delta \mathbf{B}$  (where  $\eta_m = c^2/4\pi\sigma$ , where  $c$  is the speed of light and  $\sigma$  is the conductivity of the medium), which tend to suppress the self-generation. The respective figure of merit is the *magnetic Reynolds number* [5]

$$R_m = \frac{uL}{\eta_m} = uL \frac{4\pi\sigma}{c^2}, \quad (1)$$

where  $L$  is the characteristic system size and  $u$  is the typical velocity of the medium. The threshold value for a dynamo action to commence (usually lying in the range  $R_m^{(cr)} \sim 10$ – $100$ , with  $R_m^{(cr)} \approx 17.7$  for the simplest Ponomarenko dynamo [6] discussed below) depends on the system's geometry and is rarely known exactly. It is clear, however, that the larger  $R_m$ , the more likely and more effective the dynamo action. The conductivity of astrophysical media varies greatly from  $10^{-11}$  S m<sup>-1</sup> for interstellar plasma to  $10^3$  S m<sup>-1</sup> for the solar convection shell and  $10^5$  S m<sup>-1</sup> for Earth's core, but in all of these cases the large magnetic diffusion coefficient is compensated by literally astronomical distances resulting in large magnetic Reynolds numbers, however small the conductivities are. By contrast, laboratory dynamo experiments [7] deal with naturally limited system sizes and use the conductivity and the flow velocities as the only potentially tunable parameters.

Apart from large magnetic Reynolds numbers  $R_m \gg 1$ , the emergence of a dynamo requires a number of other conditions that need to be met. In particular, certain “no-go theorems” [8] have to be overcome, such as the impossibility of a two-dimensional dynamo effect or that in a planar three-dimensional flow (i.e., with one vanishing component

of velocity). Finally, it is known that the dynamo action is greatly helped by the helicity flow, which may arise either due to the geometry of an imposed flow or due to turbulence. The latter is possible if the second figure of merit, the *hydrodynamic Reynolds number*

$$R = \frac{uL}{\nu}, \quad (2)$$

where  $\nu$  is the kinematic viscosity, is large. Separating both the velocity and magnetic field into a mean-field and fluctuating component— $\mathbf{u} = \bar{\mathbf{u}} + \delta\mathbf{u}$  and  $\mathbf{B} = \bar{\mathbf{B}} + \delta\mathbf{B}$ —and averaging over the small-scale fluctuations results in the Krause-Rädler equations [9,10] of mean-field MHD, which in the simplest case of isotropic turbulence is given by

$$\frac{\partial \bar{\mathbf{B}}}{\partial t} = \nabla \times (\bar{\mathbf{u}} \times \bar{\mathbf{B}}) + \nabla \times (\alpha \bar{\mathbf{B}}) + \xi \Delta \bar{\mathbf{B}}, \quad (3)$$

where the second term in the right-hand side is the “new” helicity term allowed in turbulent MHD ( $\alpha$  effect). If the velocity field is stationary, Eq. (3) or a similar MHD equation without helicity for nonturbulent flows becomes an eigenvalue problem for the magnetic field growth  $\mathbf{B}(\mathbf{r}, t) \propto \mathbf{B}(\mathbf{r})e^{\gamma t}$ . The existence of exponentially growing components ( $\text{Re}\gamma > 0$ ) indicates an instability towards a self-generating magnetic field (where the imaginary part  $\text{Im}\gamma > 0$  leads to the field oscillations, which have been suggested [11] by one of the authors to lead, e.g., to periodic cycles of solar magnetic activity).

Apart from the astrophysical context, there has been a tremendous interest in testing the predictions of dynamo theory and modeling a planetarylike or solarlike dynamo action in the laboratory [7,12–14]. Several impressive laboratory experiments have been carried out and are currently under way that involve setting in motion a liquid metal—sodium or gallium—with the goal to achieve large Reynolds numbers to enable the dynamo mechanism. As is obvious from Eqs. (1) and (2), this leads to the challenge of ultrafast mechanical stirring or rotating the liquid metal.

Here we propose that electronic solid-state systems may provide an alternative platform for observing magnetohydrodynamic effects. First, we list several necessary conditions of the dynamo effect in an electronic system. (i) Transport in the electron liquid should be governed by hydrodynamics; i.e., the primary momentum relaxation mechanism should be electron-electron collisions rather than impurity scattering. (ii) The system and the flow must be essentially three-dimensional. (iii) Large magnetic  $R_m \gg 1$  and/or hydrodynamic  $R \gg 1$  Reynolds numbers are required.

Hydrodynamic transport in the solid state [condition (i)] has been a subject of intense recent studies [15–19], both theoretical and experimental. On the experimental side, two widely studied platforms for hydrodynamic phenomena

are graphene [20] and Weyl semimetals (WSMs) [21–23]. Graphene, however, violates a no-go dynamo theorem—condition (ii) requiring 3D flows—and is thus of no relevance to the dynamo effect.

In what follows, we focus on magnetohydrodynamic phenomena in Weyl metals (doped Weyl semimetals). We note that, in systems with the power-law quasiparticle dispersion [24–29]  $\epsilon(\mathbf{p}) \propto |\mathbf{p}|^\beta$  with  $\beta \leq 1$ , the creation of electron-hole pairs is suppressed [30], because the energy and momentum conservation laws cannot be satisfied simultaneously for lowest-order processes. Weyl systems ( $\beta = 1$ ) may, therefore, often be considered as electron-hole plasmas with a linear particle dispersion.

A WSM generically has an even number of nodes, according to the fermion-doubling theorem [31], and electrons and holes near different nodes often behave as independent liquids. However, the simultaneous application of external electric  $\mathbf{E}$  and magnetic  $\mathbf{B}$  fields results in the quasiparticle transfer from one node to another (chiral anomaly [32–36]). For simplicity, we assume in this Letter that (a) the system has only two nodes, labeled by  $L$  and  $R$ , with the same quasiparticle dispersion, (b) the entire system is being kept at a constant temperature  $T$ , and (c) the intranodal equilibration processes are significantly faster than the internodal particle-transfer processes. This allows one to define the chemical potentials  $\mu_\alpha$  near each node  $\alpha = L, R$  and the hydrodynamic velocity  $\mathbf{u}$  of the Weyl fluid. The distribution function of the linearly dispersing quasiparticles near each node in the absence of electromagnetic fields is given by [37]  $f_\alpha(\mathbf{k}) = \{\exp[\gamma(\mathbf{u})(\pm v_F|\mathbf{k}| - \mu_\alpha - \mathbf{u} \cdot \mathbf{k})/T] + 1\}^{-1}$ , where “+” and “−” refer, respectively, to the conduction and valence bands,  $\gamma(\mathbf{u}) = (1 - u^2/v_F^2)^{1/2}$ , and  $\gamma(\mathbf{u})(\pm v_F|\mathbf{k}| - \mu_\alpha - \mathbf{u} \cdot \mathbf{k})$  is the quasiparticle dispersion in the reference frame of the moving electron liquid.

The dynamics of charge densities  $\rho_\alpha$  near node  $\alpha$ , where  $\alpha = L, R$ , are described by the continuity equations

$$\partial_t \rho_\alpha + \nabla \cdot \mathbf{j}_\alpha - \chi_\alpha \frac{ge^3}{4\pi^2 \hbar^2 c} \mathbf{E} \cdot \mathbf{B} + \frac{\rho_\alpha - \rho_{\bar{\alpha}}}{\tau_{\text{in}}} = 0, \quad (4)$$

where  $\chi_L = -1$  and  $\chi_R = +1$  are the “chiralities” of quasiparticles near nodes  $L$  and  $R$ , respectively, and  $g$  accounts for spin and possibly additional valley degeneracy;  $\bar{\alpha}$  labels the node other than  $\alpha$ ; hereinafter,  $e = -|e|$ . The first two terms in Eq. (4) match the usual continuity equation for a liquid with density  $\rho_\alpha$ ; the third term ( $\propto \mathbf{E} \cdot \mathbf{B}$ ) accounts [35,36] for the change of the electron concentration at node  $\alpha$  due to the chiral anomaly; and the last term in Eq. (4) describes internodal scattering, e.g., due to short-range-correlated quenched disorder, with the internodal scattering time  $\tau_{\text{in}}$ . The electric currents  $\mathbf{j}_{L,R}$  of the charge carriers near the two nodes are given by

$$\mathbf{j}_\alpha = \sum_\beta \sigma_{\alpha\beta} \left( \mathbf{E} + \frac{1}{c} \mathbf{u} \times \mathbf{B} - \frac{1}{e} \nabla \mu_\beta \right) - \chi_\alpha \frac{ge^2}{4\pi^2 \hbar^2 c} \mathbf{B} \mu_\alpha, \quad (5)$$

where  $\alpha, \beta = L, R$ ,  $\mu_\alpha$  is the chemical potential near node  $\alpha$ , and  $\mathbf{u}$  is the hydrodynamic velocity of the Weyl fluid. In this Letter, we assume that the imbalance of the chemical potentials between the nodes, if any, is small:  $|\mu_L - \mu_R| \ll |\mu_{L,R}|, T$ . The diagonal components  $\sigma_{LL} = \sigma_{RR}$  of the conductivity tensor  $\sigma_{\alpha\beta}$  describe the response of charge carriers near each node to the electromagnetic field; the off-diagonal entries  $\sigma_{LR} = \sigma_{RL}$  account for the drag of the quasiparticles near each node by the current near the other node. The last term in Eq. (5) describes the chiral magnetic effect [38,39], the generation of the charge current by an external magnetic field in the system in the presence of chirality imbalance:  $\mu_L - \mu_R \neq 0$ .

Equations (4) and (5), together with the relations [40]

$$\rho_{R,L} = ge \frac{\mu_{R,L}^3 + \pi^2 \mu_{R,L} T^2}{6\pi^2 v_F^3 \hbar^3} \quad (6)$$

for the charge density at node  $\alpha$  and with Maxwell equations, which involve the total charge density  $\rho = \rho_L + \rho_R$  and the current  $\mathbf{j} = \mathbf{j}_L + \mathbf{j}_R$ , constitute a closed system of equations which describes charge and current dynamics of the electron liquid in a WSM which moves with velocity  $\mathbf{u}$  in an external electromagnetic field. The motion of such a liquid may be generated by the electromagnetic fields, the temperature and chemical potential gradients, or even fast mechanical rotation of the sample.

To determine self-consistently the velocity field  $\mathbf{u}$  (which, in practice, is a tremendously difficult problem), the system of Eqs. (4)–(6) has to be complemented by the Navier-Stokes equation (derived in Supplemental Material [41])

$$\begin{aligned} \frac{w_\alpha}{v_F^2} \left( \frac{\partial}{\partial t} + \mathbf{u} \cdot \nabla \right) \mathbf{u} = & -\nabla P_\alpha - \frac{\mathbf{u}}{v_F^2} \frac{\partial P_\alpha}{\partial t} + \rho_\alpha \mathbf{E} + \frac{1}{c} \mathbf{j}_\alpha \times \mathbf{B} \\ & + \frac{\mathbf{u}}{3} \left( \frac{\partial \varepsilon}{\partial \rho} \right)_\alpha \left( \chi_\alpha \frac{ge^3}{\hbar^2 c} \mathbf{E} \cdot \mathbf{B} - \frac{\rho_\alpha - \rho_{\bar{\alpha}}}{\tau_{in}} \right) \\ & + \eta \nabla^2 \mathbf{u} + \zeta \nabla (\nabla \cdot \mathbf{u}), \end{aligned} \quad (7)$$

where  $w_\alpha = \varepsilon_\alpha + P_\alpha$  is the enthalpy of the charge carriers near node  $\alpha$  per unit volume, with [42]

$$\varepsilon_\alpha \approx g \frac{7\pi^4 T^4 + 30\pi^2 \mu_\alpha^2 T^2 + 15\mu_\alpha^4}{120\pi^2 v_F^3 \hbar^3} \quad (8)$$

and  $P_\alpha \approx (\varepsilon_\alpha/3)$  being, respectively, the contributions of node  $\alpha$  to the internal energy and pressure; the current  $\mathbf{j}_\alpha$  is given by Eq. (5);  $\eta$  and  $\zeta$  are the shear and the bulk viscosities, respectively; and the term  $\propto (\partial \varepsilon / \partial \rho)_\alpha$  accounts for the change of the energy and pressure of the Weyl liquid near node  $\alpha$  due to the internodal scattering and the chiral anomaly, where  $(\partial \varepsilon / \partial \rho)_\alpha = (3\mu_\alpha/e)(\mu_\alpha^2 + \pi^2 T^2/3\mu_\alpha^2 + \pi^2 T^2)$  for the case of an isothermal flow considered in this Letter [see Supplemental Material [41] for the discussion of the assumptions about thermalization].

In this Letter, we neglect the so-called chiral vortical effect [42], i.e., contributions to the current from the interplay of global rotations of the system and chirality imbalance ( $\mu_L - \mu_R \neq 0$ ). In the Navier-Stokes equation (7), we also neglect terms of higher orders in  $u^2/v_F^2$ . Equations (4)–(7), together with the Maxwell equations and the equations of state, in the form of Eq. (8) and  $P_\alpha = (\varepsilon_\alpha/3)$ , constitute a closed system of equations describing the dynamics of the electromagnetic fields and the electron liquid in a WSM.

Using Eq. (5), together with the Maxwell equations  $\nabla \times \mathbf{E} = -(1/c)(\partial \mathbf{B} / \partial t)$  and  $\mathbf{j}_L + \mathbf{j}_R \equiv \mathbf{j} = (c/4\pi) \nabla \times \mathbf{B}$ , where we neglected the displacement current under the assumption of a quasistationary flow, we arrive at the equation for the dynamics of the magnetic field:

$$\frac{\partial \mathbf{B}}{\partial t} = \nabla \times (\mathbf{u} \times \mathbf{B}) + \frac{c^2}{4\pi\sigma} \nabla^2 \mathbf{B} + \frac{ge^2}{4\pi^2 \hbar^2 \sigma} \nabla \times [(\mu_L - \mu_R) \mathbf{B}], \quad (9)$$

where  $\sigma = 2\sigma_{LL} + 2\sigma_{LR}$  is the conductivity of the WSM and we have taken into account that the quasiparticles have the same dispersion near the two nodes. Apart from solid-state WSMs, an equation of the form (9) with phenomenologically introduced coefficients describes the dynamics of ultra-relativistic chiral particles [43].

Equation (9) indicates that Weyl liquids allow for the helicity term for macroscopic fields without turbulence, in contrast with the conventional  $\alpha$  dynamo of Krause and Rädler [9]. However, it can appear only in the presence of an already existing field, and while, as shown below, it can further enhance magnetic field “bootstrap,” it cannot lead to generation of the field in and by itself if there is no seed field to begin with. For that, the magnetic Reynolds number (1),  $R_m$ , has to be large enough, as discussed in the introduction.

To estimate  $R_m$ , we use the equation for the Coulomb-interaction-dominated conductivity of a Weyl semimetal [44]:

$$\sigma \sim \frac{e^2 k_B T}{\hbar \hbar v_F \alpha^2}, \quad (10)$$

where the Weyl fine-structure constant is  $\alpha = e^2 / (\hbar v_F \kappa)$  and  $\kappa$  is the dielectric constant, which crucially may be rather large. While Eq. (10) has been derived neglecting screening effects [44], it should be adequate for estimates. For these purposes, we have also dropped logarithmic renormalization factors.

Let us emphasize that the dynamo effect is a *macroscopic classical phenomenon*. The effect is favored by large system sizes  $L$ , which lead to large  $R_m$ . In experiments with solid-state systems, the size  $L$  is rather limited, with centimeter-size samples being at the upper end of the range accessible for WSMs. Since the effect is not sensitive to quantum interference effects, higher temperatures  $T$  are much preferable to maximize  $R_m$ ; the room temperature  $T_{\text{room}}$  thus represents

a reasonable comparison scale. We emphasize that even at room temperature Weyl semimetals are not Maxwell gases and the quantum statistics and quantum nature of the electron-electron scattering are important, but quantum coherence is not essential for the dynamo effect. Using these length and temperature scales, we obtain the following estimate for the main figure of merit in the dynamo theory:

$$R_m \sim \frac{1}{\alpha^2} \frac{e^2}{\hbar} \frac{4\pi k_B T}{\hbar v_F c^2} u L \sim \frac{10^{-6}}{\alpha^2} \left( \frac{T}{T_{\text{room}}} \right) \times u \left[ \frac{\text{cm}}{\text{s}} \right] L [\text{cm}], \quad (11)$$

where  $u$  is the typical velocity of the flow.

Now, we turn to estimates of the hydrodynamic Reynolds number (2). The viscosity of the quasiparticles in a Weyl semimetal at temperature  $T$  may be estimated as  $\eta \sim n(T) T \tau_{\text{rel}}$ , where  $n(T)$  is the concentration of the thermally excited quasiparticles and  $\tau_{\text{rel}} \sim \hbar (\alpha^2 k_B T)^{-1}$  is the momentum relaxation time. Note that this result follows from the second-order perturbation theory in Coulomb interaction and neglects screening effects. This leads to

$$\eta \sim \frac{(k_B T)^3}{\alpha^2 \hbar^2 v_F^3}. \quad (12)$$

The motion of a Weyl-semimetal liquid is turbulent in the hydrodynamic sense when the term  $(w/v_F^2)(\mathbf{u} \cdot \nabla)\mathbf{u}$  in the Navier-Stokes equation (7) dominates the dissipative terms  $\sim \eta \nabla^2 \mathbf{u}$  that come from the viscosity of the Weyl fluid. This yields the following estimate:

$$R = \frac{w u L}{\eta v_F^2} \sim \alpha^2 \frac{k_B T}{\hbar} \frac{u L}{v_F^2} \sim 4 \alpha^2 10^{-3} \left( \frac{T}{T_{\text{room}}} \right) \times u \left[ \frac{\text{cm}}{\text{s}} \right] L [\text{cm}], \quad (13)$$

where we have used the estimate  $w \approx (7g\pi^2 T^4 / 90 \hbar^3 v_F^3) \sim [(k_B T)^4 / \hbar^3 v_F^3]$  for the specific enthalpy at high temperatures.

We note in this context that the viscosity of a Fermi liquid at temperature  $T$  may be estimated as  $\eta \sim \varepsilon_F^5 / (T^2 \hbar^2 v_F^3)$ , where  $\varepsilon_F$  and  $v_F$  are the Fermi energy and velocity, respectively. Because the hydrodynamic Reynolds number  $R \sim (T^2 / v_F^2 \varepsilon_F \hbar)$  gets rapidly suppressed with increasing the Fermi energy  $\varepsilon_F$ , topological semimetals are indeed a favorable platform for achieving electronic turbulence as compared to “conventional” hydrodynamic metals.

Naturally, the geometry and the magnitude of the velocity field  $u$  much depend on the mechanism to stir up hydrodynamic motion and follow from the solution of the Navier-Stokes equations, which is a challenging task in most cases. Furthermore, since the observation of a phenomenon of this kind has never been attempted in solid-state materials, specific experimental techniques for achieving high hydrodynamic flows in the most efficient way still deserve further investigation—pulsed fields (in particular

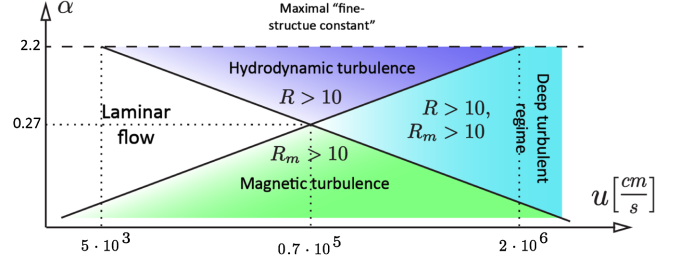


FIG. 1. Flow regimes for the electron liquid in a Weyl semimetal on the diagram “fine-structure constant”  $\alpha = (e^2 / \chi \hbar v_F)$  vs flow velocity  $u$  (log-log scale) for the room temperature  $T = T_{\text{room}} = 300$  K and the Fermi velocity  $v_F = 10^8$  (cm/s). The maximum value of the fine-structure constant is  $\alpha_{\text{max}} = (e^2 / \hbar v_F) \approx 2.2$ .

orbital-angular-momentum pulses [45] in a cylindrical geometry), crossed electric and magnetic fields, or just a rapid rotation of the sample are all possibilities to consider. While below we consider in detail one of the standard and simplest dynamo models, we emphasize immediately that the estimates (11) and (13) are not prohibitive; and it is conceivable that relatively large magnetic Reynolds numbers, necessary for the dynamo to commence, are achievable for realistic flow velocities with  $u$  of the order of 1 km/s or greater (especially considering that the dielectric constant may be as high as  $\chi \sim 50$  in WSMs); cf. Fig. 1.

Now, we discuss a specific model of the dynamo effect—the so-called kinematic Ponomarenko dynamo [6,8]—with an eye on how the terms in MHD equations, descending from the chiral anomaly, change the effect. The Ponomarenko dynamo does not necessarily represent the most experimentally realistic setup, but it does represent the simplest textbook model, which contains the key qualitative features of a dynamo mechanism and is amenable to analytical analysis.

In order for a dynamo action to occur, the magnetic Reynolds number must exceed a critical value  $R_m^c$  [46]. The purpose of the calculation below is to obtain the dependence of the critical Reynolds number  $R_m^c$  on the helicity term. For simplicity, we neglect the time dependence of the chemical-potential difference  $\mu_L - \mu_R$  on the times we consider.

We rewrite Eq. (9) as

$$\frac{\partial \mathbf{B}}{\partial t} = \nabla \times (\mathbf{u} \times \mathbf{B}) + \frac{c^2}{4\pi\sigma} \nabla^2 \mathbf{B} + \xi \nabla \times \mathbf{B}, \quad (14)$$

where  $\xi = ge^2(\mu_L - \mu_R) / (4\pi^2 \hbar^2 \sigma)$ . We consider a cylindrical geometry of the sample with a flow field  $\mathbf{u} = (0, r\Omega, u_0)$ , where  $\Omega$  and  $u_0$  are constants, for  $r \leq a$  and  $\mathbf{u} = 0$  for  $r > a$  [46]. Plugging the ansatz  $\mathbf{B}(r, \theta, z, t) = \mathbf{B}(r) e^{i(n\theta - kz) + \gamma t}$  into (9), the components of the magnetic field  $B_{\pm} = B_r \pm iB_{\theta}$  satisfy the equations

$$y^2 B''_{\pm} + y B'_{\pm} = [q^2 y^2 + (n \pm 1)^2] B_{\pm} - \delta [n y B'_{\mp} \mp n(n \mp 1) B_{\mp} \pm k^2 a^2 y^2 B_{\pm} \mp q^2 y^2 B_r] \quad (15)$$

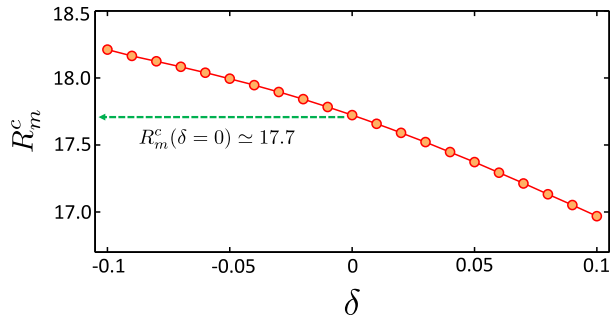


FIG. 2. The critical magnetic Reynolds number  $R_m^c$  of the  $n = 1$  kinematic Ponomarenko dynamo as a function of the helicity parameter  $\delta = 4\pi\sigma\xi/kc^2$ , with  $k$  being the wave vector of the dynamo instability.  $R_m^c \simeq 17.7$  is the critical value for the dynamo in the absence of helicity. We note that a self-exciting dynamo will always correspond to the chirality with a lower critical Reynolds number. The chiral anomaly, thus, always aids the dynamo effect.

for  $y = r/a \leq 1$  and

$$y^2 B''_{\pm} + y B'_{\pm} = [s^2 y^2 + (n \pm 1)^2] B_{\pm} \quad (16)$$

for  $y > 1$ , where  $B'_{\pm}$  ( $B''_{\pm}$ ) is the first (second) derivative with respect to  $y$ ;  $\delta = 4\pi\sigma\xi/kc^2$ ,  $q^2 = k^2 a^2 + \gamma\tau_R + i(n\Omega - ku_0)$ , and  $s^2 = k^2 a^2 + \gamma\tau_R$ , where  $\tau_R = 4\pi\sigma a^2/c^2$  is the time scale of the magnetic field diffusion.

For each mode  $n$ , the magnetic field starts to grow exponentially when  $\text{Re}(\gamma) > 0$ , which occurs if the magnetic Reynolds number exceeds a critical value  $R_m^c$ . In the absence of helicity ( $\delta = 0$ ), Eq. (14) reduces to the conventional dynamo equation and the  $n = 0$  mode is not excited for an arbitrary intensity of the flow [46]. For nonzero helicity, we solved the inhomogeneous equations (15) and (16) with appropriate boundary conditions imposed [41] to obtain the dispersion relation for the dynamo mode. The obtained values of  $R_m^c$  for a dynamo with  $n = 1$  and a particular direction of wave vector  $\mathbf{k}$  (the  $z$  axis) are shown in Fig. 2. The  $n = 1$  mode is the leading mode, where the dynamo action commences first, and for which the critical magnetic Reynolds number is the smallest and potentially within reach for actual Weyl systems. In the absence of helicity (i.e., if  $\delta = 0$ ), it is known to be  $R_m^c \simeq 17.7$  [46]. Interestingly enough, the helicity  $\delta > 0$  reduces the critical value of the magnetic Reynolds number for the  $n = 1$  mode and helps the dynamo action to occur for  $R_m^c < 17.7$ . Because dynamo flows with various directions of  $\mathbf{k}$  may emerge spontaneously in a turbulent liquid, the presence of helicity (a consequence of the chiral anomaly) would generically aid the dynamo bootstrap in any geometry of the flow.

In conclusion, this Letter proposes hydrodynamic Weyl semimetals as a host to electronic turbulence and/or a dynamo effect. We derived the Navier-Stokes equations (7) and equations of magnetohydrodynamics (9) and estimated

two key figures of merit—the hydrodynamic and magnetic Reynolds numbers. Figure 1 summarizes our findings and shows that both turbulence and the dynamo mechanism are, in principle, experimentally achievable. However, many interesting questions remain, such as experimental signatures of the turbulent electronic motion and the role of “new” terms in the Navier-Stokes equations, descending from the quantum chiral anomaly. Finally, we mention that, while three-dimensional Dirac materials are indeed interesting from the perspective of realizing the dynamo bootstrap, a number of other electronic materials may also serve as platforms to realize the effect. For example, electronic metals near critical points (e.g., right above a superconducting transition) represent a promising system to look at in this context (from the perspective of achieving both hydrodynamic flows and large Reynolds numbers) and could pave the way to simulating in solid-state materials the effect of magnetic field self-excitation—a remarkable phenomenon, usually delegated to the fields of geophysics, astrophysics, and cosmology.

We are grateful to Matthew Foster, Anton Burkov, and Aydin Keser for useful discussions. This research was supported by NSF DMR-1613029 (S. S.), the DOE-BES (DESC0001911) (V. G.), and the Simons Foundation (V. G.). M. K. acknowledges the support from the Sharif University of Technology under Grant No. G690208.

- 
- [1] J. Larmor, How could a rotating body such as the Sun become a magnet?, *Rep. Br. Assoc.* **87**, 159 (1919).
  - [2] A. A. Ruzmaikin, D. D. Sokoloff, and Ya. B. Zeldovich, *The Almighty Chance*, Lecture Notes in Physics (World Scientific, Singapore, 1990).
  - [3] A. D. Gilbert, in *Handbook of Mathematical Fluid Dynamics*, edited by S. Friedlander and D. Serre (Elsevier Science BV, Amsterdam, 2003), Vol. 2, pp. 355–441.
  - [4] A. D. Gilbert, in *Mathematical Aspects of Natural Dynamos*, edited by E. Dormy and A. M. Soward (CRC Press, Boca Raton, 2007), Chap. 1.
  - [5] L. D. Landau and E. M. Lifshitz, *Fluid Mechanics*, 2nd ed., Course of Theoretical Physics (Butterworth-Heinemann, London, 1987), Vol. 6.
  - [6] Yu. B. Ponomarenko, On the theory of hydromagnetic dynamo, *J. Appl. Mech. Tech. Phys.* **14**, 775 (1973).
  - [7] D. P. Lathrop and C. B. Forest, Magnetic dynamos in the lab, *Phys. Today* **64**, No. 7, 40 (2011).
  - [8] C. A. Jones, *Course 2: Dynamo Theory*, Lecture Notes of the Les Houches Summer School 2007, edited by Ph. Cardin and L. F. Cugliandolo, Session LXXXVIII (Elsevier, New York, 2008).
  - [9] F. Krause and K-H. Rädler, *Mean Field Magnetohydrodynamics and Dynamo Theory* (Pergamon, New York, 1980).
  - [10] E. N. Parker, Hydromagnetic dynamo models, *Astrophys. J.* **122**, 293 (1955).
  - [11] V. M. Galitski and D. D. Sokoloff, Kinematic dynamo wave in the vicinity of the solar poles, *Geophys. Astrophys. Fluid Dyn.* **91**, 147 (1999).

- [12] A. Gailitis, O. Lielausis, S. Dement'ev, E. Platacis, A. Cifersons, G. Gerbeth, T. Gundrum, F. Stefani, M. Christen, H. Hänel, and G. Will, Detection of a Flow Induced Magnetic Field Eigenmode in the Riga Dynamo Facility, *Phys. Rev. Lett.* **84**, 4365 (2000).
- [13] E. J. Spence, M. D. Nornberg, C. M. Jacobson, C. A. Parada, N. Z. Taylor, R. D. Kendrick, and C. B. Forest, Turbulent Diamagnetism in Flowing Liquid Sodium, *Phys. Rev. Lett.* **98**, 164503 (2007).
- [14] R. Monchaux, M. Berhanu, M. Bourgoïn, M. Moulin, Ph. Odier, J.-F. Pinton, R. Volk, S. Fauve, N. Mordant, F. Pétrélis, A. Chiffaudel, F. Daviaud, B. Dubrulle, C. Gasquet, L. Marié, and F. Ravelet, Generation of a Magnetic Field by Dynamo Action in a Turbulent Flow of Liquid Sodium, *Phys. Rev. Lett.* **98**, 044502 (2007).
- [15] A. V. Andreev, Steven A. Kivelson, and B. Spivak, Hydrodynamic Description of Transport in Strongly Correlated Electron Systems, *Phys. Rev. Lett.* **106**, 256804 (2011).
- [16] A. Lucas and S. A. Hartnoll, Resistivity bound for hydrodynamic bad metals, *Proc. Natl. Acad. Sci. U.S.A.* **114**, 11344 (2017).
- [17] A. Lucas and S. Das Sarma, Electronic sound modes and plasmons in hydrodynamic two-dimensional metals, *Phys. Rev. B* **97**, 115449 (2018).
- [18] X.-Y. Song, C.-M. Jian, and L. Balents, A Strongly Correlated Metal Built from Sachdev-Ye-Kitaev Models, *Phys. Rev. Lett.* **119**, 216601 (2017).
- [19] S. A. Hartnoll, A. Lucas, and S. Sachdev, *Holographic Quantum Matter* (MIT, Cambridge, MA, 2018).
- [20] R. Krishna Kumar, D. A. Bandurin, F. M. D. Pellegrino, Y. Cao, A. Principi, H. Guo, G. H. Auton, M. Ben Shalom, L. A. Ponomarenko, G. Falkovich, K. Watanabe, T. Taniguchi, I. V. Grigorieva, L. S. Levitov, M. Polini, and A. K. Geim, Superballistic flow of viscous electron fluid through graphene constrictions, *Nat. Phys.* **13**, 1182 (2017).
- [21] J. Gooth, A. C. Niemann, T. Meng, A. G. Grushin, K. Landsteiner, B. Gotsmann, F. Menges, M. Schmidt, C. Shekhar, V. Sueb, C. F. R. Huehne, B. Rellinghaus, B. Yan, and K. Nielsch, Experimental signatures of the mixed axial-gravitational anomaly in the Weyl semimetal NbP, *Nature (London)* **547**, 324 (2017).
- [22] J. Gooth, F. Menges, C. Shekhar, V. Sueb, N. Kumar, Y. Sun, U. Drechsler, R. Zierold, C. Felser, and B. Gotsmann, Electrical and thermal transport at the Planckian bound of dissipation in the hydrodynamic electron fluid of WP2, [arXiv:1706.05925](https://arxiv.org/abs/1706.05925).
- [23] C. Fu, T. Scaffidi, J. Waissman, Y. Sun, R. Saha, S. J. Watzman, A. K. Srivastava, G. Li, W. Schnelle, P. Werner, M. E. Kamminga, S. Sachdev, S. S. P. Parkin, S. A. Hartnoll, C. Felser, and J. Gooth, Thermoelectric signatures of the electron-phonon fluid in PtSn4, [arXiv:1802.09468](https://arxiv.org/abs/1802.09468).
- [24] P. Richerme, Z.-X. Gong, A. Lee, C. Senko, J. Smith, M. Foss-Feig, S. Michalakakis, A. V. Gorshkov, and C. Monroe, Non-local propagation of correlations in quantum systems with long-range interactions, *Nature (London)* **511**, 198 (2014).
- [25] R. Islam, C. Senko, W. C. Campbell, S. Korenblit, J. Smith, A. Lee, E. E. Edwards, C.-C. J. Wang, J. K. Freericks, and C. Monroe, Emergence and frustration of magnetism with variable-range interactions in a quantum simulator, *Science* **340**, 583 (2013).
- [26] P. Jurcevic, B. P. Lanyon, P. Hauke, C. Hempel, P. Zoller, R. Blatt, and C. F. Roos, Quasiparticle engineering and entanglement propagation in a quantum many-body system, *Nature (London)* **511**, 202 (2014).
- [27] P. Jurcevic, P. Hauke, C. Maier, C. Hempel, B. P. Lanyon, R. Blatt, and C. F. Roos, Spectroscopy of Interacting Quasiparticles in Trapped Ions, *Phys. Rev. Lett.* **115**, 100501 (2015).
- [28] T. Nagao, S. Yaginuma, T. Inaoka, and T. Sakurai, One-Dimensional Plasmon in an Atomic-Scale Metal Wire, *Phys. Rev. Lett.* **97**, 116802 (2006).
- [29] A. A. Burkov, Topological semimetals, *Nat. Mater.* **15**, 1145 (2016).
- [30] M. S. Foster and I. L. Aleiner, Slow imbalance relaxation and thermoelectric transport in graphene, *Phys. Rev. B* **79**, 085415 (2009).
- [31] H. B. Nielsen and M. Ninomiya, Absence of neutrinos on a lattice: (I). Proof by homotopy theory, *Nucl. Phys.* **B185**, 20 (1981).
- [32] S. L. Adler, Axial-vector vertex in spinor electrodynamics, *Phys. Rev.* **177**, 2426 (1969).
- [33] J. S. Bell and R. Jackiw, A pcac puzzle:  $\pi^0 \rightarrow \gamma\gamma$  in the  $s$ -model, *Nuovo Cimento A* **60**, 47 (1969).
- [34] D. T. Son and B. Z. Spivak, Chiral anomaly and classical negative magnetoresistance of Weyl metals, *Phys. Rev. B* **88**, 104412 (2013).
- [35] A. A. Burkov, Weyl metals, *Annu. Rev. Condens. Matter Phys.* **9**, 359 (2018).
- [36] A. A. Burkov, Chiral Anomaly and Diffusive Magnetotransport in Weyl Metals, *Phys. Rev. Lett.* **113**, 247203 (2014).
- [37] B. N. Narozhny, I. V. Gornyi, A. D. Mirlin, and J. Schmalian, Hydrodynamic approach to electronic transport in graphene, *Ann. Phys. (Berlin)* **529**, 1700043 (2017).
- [38] K. Fukushima, D. E. Kharzeev, and H. J. Warringa, Chiral magnetic effect, *Phys. Rev. D* **78**, 074033 (2008).
- [39] D. Kharzeev, K. Landsteiner, A. Schmitt, and H.-U. Yee, in *Strongly Interacting Matter in Magnetic Fields*, Lecture Notes in Physics Vol. 871 (Springer Verlag, Berlin, 2013).
- [40] Y. I. Rodionov and S. V. Syzranov, Conductivity of a Weyl semimetal with donor and acceptor impurities, *Phys. Rev. B* **91**, 195107 (2015).
- [41] See Supplemental Material at <http://link.aps.org/supplemental/10.1103/PhysRevLett.121.176603> for a detailed derivation of the Navier-Stokes equation and Ponomarenko dynamo in the presence of helicity terms.
- [42] E. V. Gorbar, V. A. Miransky, I. A. Shovkovy, and P. O. Sukhachov, Consistent hydrodynamic theory of chiral electrons in Weyl semimetals, *Phys. Rev. B* **97**, 121105 (2018).
- [43] N. Yamamoto, Chiral transport of neutrinos in supernovae: Neutrino-induced fluid helicity and helical plasma instability, *Phys. Rev. D* **93**, 065017 (2016).
- [44] P. Hosur, S. A. Parameswaran, and A. Vishwanath, Charge Transport in Weyl Semimetals, *Phys. Rev. Lett.* **108**, 046602 (2012).
- [45] L. Allen, M. W. Beijersbergen, R. J. C. Spreeuw, and J. P. Woerdman, Orbital angular momentum of light and the transformation of Laguerre-Gaussian laser modes, *Phys. Rev. A* **45**, 8185 (1992).
- [46] R. Fitzpatrick, *Plasma Physics: An Introduction* (Taylor & Francis, London, 2015).